Complexes of syndapin II with dynamin II promote vesicle formation at the trans-Golgi network

Michael M. Kessels[1,*], Jiaxin Dong[2,*,‡], Wibke Leibig[1,§], Peter Westermann[2,¶] and Britta Qualmann[1,#,]**

[1]Department of Neurochemistry and Molecular Biology, AG Membrane Trafficking and Cytoskeleton, Leibniz Institute for Neurobiology, 39118 Magdeburg, Germany
[2]Department of Cell Growth and Differentiation, Max-Delbrück-Centre for Molecular Medicine, 13092 Berlin-Buch, Germany
*These authors contributed equally to this work
‡Present address: Department of Cell Biology and Physiology, Washington University School of Medicine, St Louis, MO 63110, USA
§Present address: Department of Internal Medicin II, Technical University of Munich, 81675 Munich, Germany
¶Present address: Wodanstrasse 4, 13127 Berlin, Germany
**Present address: Research Group Celll Biology, Leibritz Institute for Neurobiology, 39118 Magoleburg, Germany
#Author for correspondence (e-mail: Britta.Qualmann@ifn-magdeburg.de)

Accepted 5 January 2006
Journal of Cell Science 119, 1504-1516 Published by The Company of Biologists 2006
doi:10.1242/jcs.02877

Summary

The role of dynamin and so-called accessory proteins in endocytosis is well established. However, molecular details of the function(s) of dynamin II at the Golgi are largely unclear. We demonstrate that the ubiquitously expressed syndapin II isoform interacts with the proline-rich domain (PRD) of dynamin II through its Src-homology 3 (SH3) domain. Co-immunoprecipitation of endogenous syndapin II and dynamin II, and successful reconstitutions of such complexes at membranes in COS-7 cells, show the in vivo relevance of the interaction. Syndapin II can associate with Golgi membranes and this association increases upon Golgi exit block. Brefeldin A treatment clearly shows that the observed perinuclear localization of syndapin II co-localizing with syntaxin 6 reflects the Golgi complex and that it requires functional integrity of the Golgi. Syndapins are crucial for Golgi vesicle formation because anti-syndapin antibodies, used either in in vitro reconstitutions or in living cells, inhibited this process. Both types of assays additionally revealed the essential role of syndapin II SH3 interactions with the dynamin II PRD in vesicle formation. An excess of the syndapin SH3 domain strongly inhibited budding from Golgi membranes in vitro. Likewise, overexpression of the syndapin SH3 domain or of a dynamin II variant incapable of associating with syndapin II (dynamin IIΔPRD) impaired trafficking of vesicular stomatitis virus glycoprotein (VSVG)-GFP in vivo. By contrast, full-length syndapin II-l had no negative effect, and instead promoted VSVG-GFP export from the Golgi. Importantly, a cytosolic fraction containing endogenous syndapin-dynamin complexes was sufficient to promote vesicle formation from Golgi membranes in a syndapin-dependent manner. Thus, syndapin-dynamin complexes are crucial and sufficient to promote vesicle formation from the trans-Golgi network.

Key words: Membrane trafficking, Syndapin, PACSIN, Dynamin, Vesicle formation, Golgi

Introduction

Vesicle formation from the different donor membranes within a cell is a difficult task that requires specific complex protein machineries. Syndapins are a family of Src-homology 3 (SH3) domain-containing proteins and comprise: the syndapin I isoform, which is neuronal; the syndapin II isoform, which is ubiquitously expressed and exists as several splice variants, including the 56 kDa version (syndapin II-l), which seems to be the most abundant; and the syndapin III isoform, which is predominantly muscle specific (Kessels and Qualmann, 2004). The syndapins belong to the so-called accessory proteins in endocytosis and interact with the large GTPase dynamin, which has a crucial role in endocytic vesicle fission (for reviews, see Hinshaw, 2000; Qualmann and Kessels, 2002; Slepnev and De Camilli, 2000). As dynamin works in close conjunction with SH3-domain-containing accessory proteins, an excess of syndapin SH3 domains inhibits endocytic vesicle formation in in vitro reconstitution assays (Simpson et al., 1999) as well as in vivo (Qualmann and Kelly, 2000). Quantitative electron microscopical analyses of cells with inhibited endocytosis showed an increase of clathrin-coated structures (da Costa et al., 2003). In in vitro reconstitution assays, the SH3-domain-mediated block could specifically be assigned to the final dynamin-dependent fission step of vesicle formation (Simpson et al., 1999). Furthermore, a set of experiments indicated that syndapins and their protein interactions are crucial for the process of endocytic vesicle formation (Kessels and Qualmann, 2002; Braun et al., 2005).

Further analyses of syndapin functions strongly suggested that syndapins are also capable of interfacing with the actin polymerization machinery Arp2/3 complex through a direct binding of its catalytic activator N-WASP. In living cells, this interaction manifests in an increase of actin polymerization dependent on the Arp2/3 complex (Qualmann and Kelly, 2000; Kessels and Qualmann, 2002; da Costa et al., 2003). Syndapins might thus help spatially and temporally to organize and control the process of endocytic vesicle formation within the environment of the cortical actin cytoskeleton (reviewed by Kessels and Qualmann, 2004), which might support the vesicle formation process by several means (Qualmann et al., 2000; Qualmann and Kessels, 2002).

Our most recent analyses suggest that syndapins also have an

Journal of Cell Science

Journal of Cell Science

important role in vesicle formation from the endosomal recycling compartment (Braun et al., 2005). Here, we show that syndapin II localizes to the Golgi and interacts with the proline-rich domain (PRD) of dynamin II. This dynamin isoform is predominantly found in peripheral tissues and seems to be of importance for Golgi vesicle formation (McNiven et al., 2000; Praefcke and McMahon, 2004). In accordance with its cellular localization (Maier et al., 1996), dynamin-specific antibodies inhibited vesicle formation at Golgi cisternae in vitro (Jones et al., 1998; J. Dong, Impact of dynamin II domains on the function of dynamin II in vesicle formation at the trans-Golgi network, PhD thesis, Free University of Berlin, 2001) and expression of dominant-negative dynamin II constructs inhibited membrane protein export from the Golgi complex and disrupted Golgi structure (Kreitzer et al., 2000; Cao et al., 2000). Our data show that complexes of syndapin II with dynamin II have an essential role in transport vesicle formation from the Golgi, suggesting a striking similarity between the molecular mechanisms of vesicle formation at the plasma membrane and the Golgi complex.

Results

Syndapin II co-fractionates with dynamin II

We have recently demonstrated that syndapins are crucial for vesicle formation from the plasma membrane, a function that also crucially depends on the syndapin interaction partner dynamin, and that syndapins furthermore have a role in exit from the recycling compartment together with EHD proteins (Braun et al., 2005). These data suggest that syndapins have a more general role in vesicle formation processes. Vesicle formation from the trans-Golgi network (TGN) seems somewhat similar to vesicle formation from the plasma membrane (Kessels and Qualmann, 2004; Kessels and Qualmann, 2005). We thus asked whether syndapins might form complexes with dynamin II, because this isoform of the dynamin family has been described as being involved in vesicle formation from the TGN (Jones et al., 1998; Kreitzer et al., 2000; Cao et al., 2000; J. Dong, PhD thesis). Analyses of HepG2 cell extracts showed that dynamin II and the ubiquitously expressed syndapin II isoform co-fractionate in 10-30% glycerol gradients (Fig. 1). Dynamin II distributed through the gradient with major fractions in the range between 100 and 400 kDa, suggesting the existence of a variety of dynamin II complexes (Fig. 1A). Most syndapin II can be found in fractions 6-8, corresponding to about 120-200 kDa (Fig. 1B). Dynamin also showed its highest abundance in these fractions (Fig. 1A). Little syndapin II can be found in fraction 9, which roughly corresponds to the calculated molecular mass of a single syndapin II (51 kDa and 56 kDa, depending on the splice variant) (Fig. 1B). These observations suggest that syndapins exist mostly in higher order protein complexes, which are at least partially stable in glycerol gradients and might contain dynamin II.

Syndapin II can associate with various dynamin II splice isoforms in a direct interaction dependent on the SH3 domain and the PRD

We next directly addressed whether syndapin II binds to dynamin II by affinity purification experiments with immobilized syndapin II SH3 domain – the probable binding interface suggested from studies of syndapin I and II binding to the dynamin I isoform (Qualmann et al., 1999; Qualmann and Kelly, 2000). Green fluorescent protein (GFP)-tagged

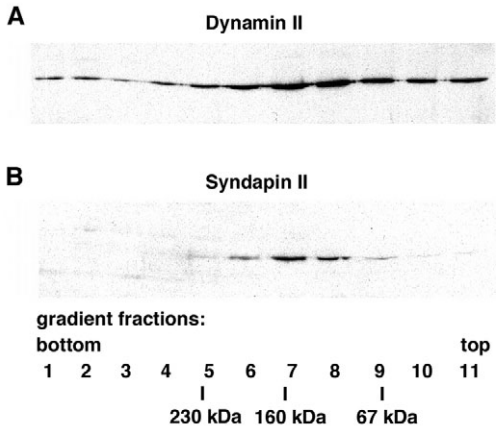

Fig. 1. Co-sedimentation of dynamin II and syndapin II. Cytosolic proteins from HepG2 cells were centrifuged through a 10-30% glycerol gradient and fractions were analyzed by immunoblotting with the anti-dynamin II antibody C12 (A) and the anti-syndapin II antibody 3685 (B). The corresponding molecular masses were determined by positions of the marker protein catalase (230 kDa), aldolase (160 kDa) and bovine serum albumin (67 kDa), run on parallel gradients.

dynamin II expressed in HEK293 cells was efficiently co-precipitated by the GST-syndapin II SH3 domain, but not by GST alone (Fig. 2A). The interaction was dynamin II specific, because a GFP control was not precipitated. The association of syndapin II with dynamin II was observed irrespective of dynamin II alternative splicing. Syndapin II interacted about equally strongly with dynamin IIaa-GFP, dynamin IIab-GFP and dynamin IIIbb-GFP (Fig. 2A). Since no binding to dynamin IIaaΔPRD-GFP was detected, we can conclude that the association requires the PRD of dynamin II (Fig. 2A).

To demonstrate that the PRD of dynamin II is not only required but is also sufficient for binding, we offered HepG2 cell lysates to immobilized dynamin II PRD fusion proteins. Endogenous syndapin II was specifically and effectively precipitated by the dynamin II PRD but not by the PH domain used as a control (Fig. 2B). Similar results were obtained with rat brain extracts (not shown).

The fact that the syndapin II SH3 domain and the PRD of dynamin II were sufficient for the association suggested a direct interaction between the SH3 domain and the PXXP motif within the PRD. We thus performed in vitro reconstitutions with purified GST-syndapin II SH3 domain and immobilized S-PRD. The observed complex formation (Fig. 2C) indicated a stable and direct association of the syndapin II SH3 domain with the PRD of dynamin II in vitro.

Syndapin II and dynamin II co-localize and interact in vivo

To obtain some hints on whether and where syndapin II and dynamin II interact in vivo, we performed immunofluorescence experiments with Xpress-tagged syndapin II-l and dynamin IIaa-GFP, a splice variant of dynamin II that had been demonstrated to localize to the Golgi complex (Cao et al., 1998). As shown in Fig. 3, we observed a clear co-localization of dynamin II and syndapin II within cells. This co-localization was observable both in perinuclear areas as well as in the

Journal of Cell Science

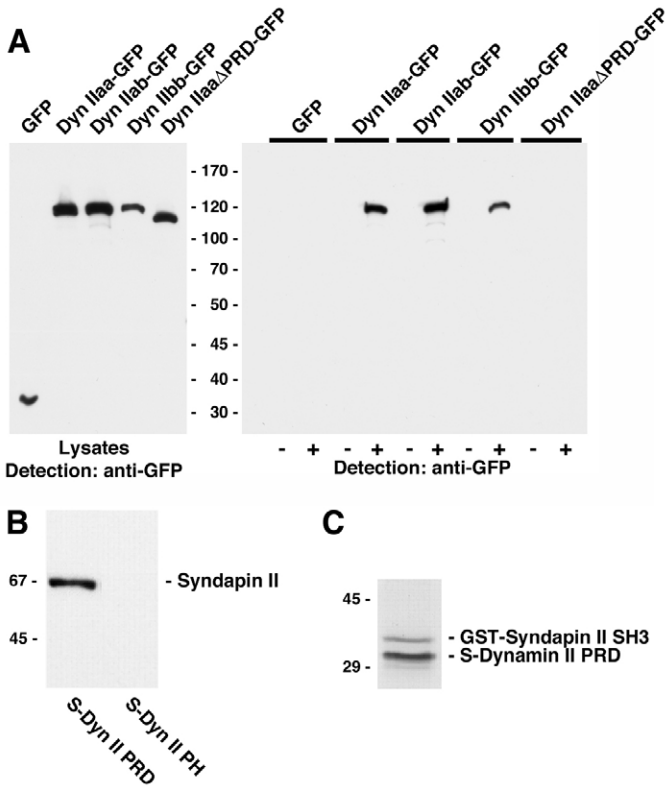

Fig. 2. Syndapin II interacts with different splice variants of dynamin II through direct association between the SH3 domain and the PRD. (A) Immunoblot analyses of co-precipitations of GFP-tagged full-length and truncated dynamin (Dyn) II proteins overexpressed in HEK293 cells with immobilized GST (–) or a GST fusion protein of the SH3 domain of syndapin II (+). Lysates as well as co-precipitated proteins were analyzed by immunoblotting with anti-GFP antibodies. The three GFP-tagged dynamin II splice variants were all specifically co-precipitated by the syndapin II SH3 domain, whereas dynamin II lacking the PRD or GFP alone did not bind (right panel). (B) A S-peptide-tagged fusion protein containing the dynamin II PRD specifically binds endogenous syndapin II from HepG2 cell extracts, whereas a related fusion protein comprising the dynamin II PH domain does not. Eluates were analyzed by immunoblotting with anti-syndapin II antibody 2521. (C) In vitro reconstitution of the interaction with purified fusion proteins (GST-Syndapin II SH3 and S-Dynamin II PRD) demonstrates that the association of both proteins is direct. SDS-eluted proteins were analyzed by immunoblotting using the anti-dynamin II antibody C12 and anti-GST antibodies to detect the S-PRD and the GST-SH3 fusion proteins, respectively.

periphery of the cells. Peripheral accumulations of both proteins were especially observed in cell protrusions that were of lamellipodial appearance (Fig. 3).

The spatial overlap of syndapin II and dynamin II prompted us to analyze complex formation of both proteins in vivo. Immunoprecipitation experiments showed that anti-syndapin II antibodies not only precipitated endogenous syndapin II from HepG2 cell extracts but also co-immunoprecipitated endogenous dynamin II (Fig. 4A). Neither dynamin II nor syndapin II associated with control IgGs. Co-immunoprecipitations of endogenous syndapin-dynamin complexes were also observed with the anti-dynamin II antibody sc-6401 (Fig. 4A).

The immunoprecipitation experiments also support the conclusion from the in vitro analyses of the protein domains involved in the association (Fig. 2). The anti-dynamin II PRD antibody C12 effectively precipitated dynamin II. Virtually no dynamin II remained in the supernatant (Fig. 4B). However, the association of the C12 antibody with the dynamin II PRD prevented the association of syndapin II, which was undetectable in the immunoprecipitates (Fig. 4A).

Syndapin II was completely immunoprecipitated by anti-syndapin II antibodies as well as by the anti-dynamin II antibody sc-6401 (Fig. 4A,B), indicating that syndapin II is predominantly found in complex with dynamin II. However, dynamin II seems to be present in a molar excess over syndapin II because a sub-pool of dynamin II was still readily detectable in the supernatant after immunoprecipitation with anti-syndapin II antibodies (Fig. 4B).

We next evaluated whether syndapin II and dynamin II could form complexes in close proximity to membranes. We used a targeting system that we have developed for in vivo reconstitution of protein complexes at defined intracellular membranes (Kessels and Qualmann, 2002). It allows for protein incorporations into the outer mitochondrial membrane in such a way that proteins of interest face the cytoplasm (Kessels and Qualmann, 2002). Indeed, both mito-syndapin II-l and the corresponding P480L mutant were efficiently targeted to mitochondria, as demonstrated by a very high degree of co-localization with MitoTracker® (see Fig. 5A for an example).

We next co-expressed different dynamin II splice variants. If the interaction between syndapin II and dynamin II shown in vitro (Fig. 2) is of high affinity in vivo, the co-expressed GFP-dynamin fusion proteins should be recruited to syndapin-coated mitochondria. When dynamin IIaa-GFP was co-expressed, it indeed adopted a mitochondrial localization pattern (Fig. 5B,E) that overlapped exactly with mito-syndapin II-l and MitoTracker® (Fig. 5C,F, respectively). Similar to the results in vitro (Fig. 2A), formation of syndapin II-l complexes with dynamin II were not restricted to individual splice forms in vivo. Similar to our experiments with dynamin IIaa, we observed a very efficient recruitment of dynamin IIab-GFP (Fig. 5G-I) and dynamin IIbb-GFP (Fig. 5J-L) to syndapin II-coated mitochondria, as also evidenced by a co-localization of dynamin IIab and dynamin IIbb with MitoTracker® (data not shown). By contrast, all three GPF-tagged dynamin II splice variants tested did not co-localize with mitochondria when transfected alone (data not shown). Since mito-syndapin II-l also recruited Myc-tagged dynamins but did not recruit GFP (data not shown), the targeting was not dependent on the tag but was dynamin specific. In cells cotransfected with the mutant mito-syndapin II-l P480L (Fig. 5M), no mitochondrial recruitment was observable, but dynamin IIaa-GFP (Fig. 5N) showed a rather diffuse localization. Also, no recruitment of dynamin IIab-GFP and dynamin IIbb-GFP to mitochondria decorated with mito-syndapin II-l P480L was observed (data not shown). Thus, complex formation between syndapin II and dynamin II depends on the syndapin II SH3 domain in vivo.

The intracellular distribution of syndapin II includes an association with Golgi membranes

As interactions between syndapin II and dynamin II within the cytosol and at membranes could solely represent the established endocytic role of syndapins, we next analyzed the

Journal of Cell Science

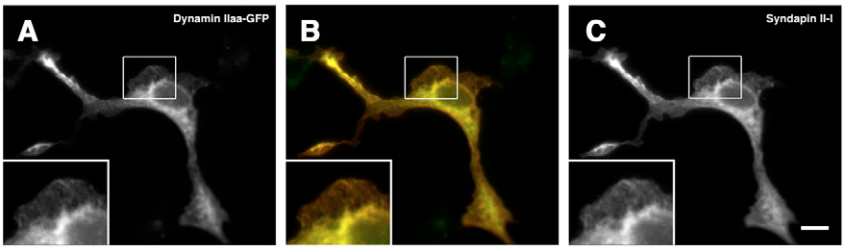

Fig. 3. Co-localization of dynamin IIaa-GFP and Flag-syndapin II-l. (A-C) COS-7 cells cotransfected with dynamin IIaa-GFP and epitope-tagged syndapin II-l detected by GFP fluorescence (A) and anti-Flag immunostaining (C), respectively, show a complete spatial overlap of both proteins in the merged image (B; syndapin in red and dynamin in green; overlap appears yellow). Co-localization can be observed both at the perinuclear area and in the periphery of the cells. Insets represent twofold enlargements of boxed areas. Bar, 10 μm.

intracellular distribution of endogenous syndapin II more closely. Earlier analyses have focused on the localization of syndapin II to cortical regions of PC12 cells and to areas of the plasma membrane forming filopodia and lamellipodia (Qualmann and Kelly, 2000). In addition, there seems to be a large cytosolic and also a perinuclear pool of the protein. Fractionation of HepG2 cell extracts showed that syndapin II is predominantly in the cytoplasm (not shown). However, a minor portion was bound to membranes stable enough to float up on 10-30% glycerol gradients (Fig. 1; fractions 10 and 11). When light membranes isolated from HepG2 cells were floated through 1.18 M sucrose – an efficient way to isolate Golgi-enriched membranes that are free of endoplasmic reticulum (ER) and endosomal contaminations (Westermann et al., 1996) – syndapin II was found both bound to light membranes and to Golgi-enriched membranes, whereas membranes of a higher density were found not to be associated with syndapin II (Fig. 6A). This observation underlines the specificity of membrane binding of syndapin II.

A pre-incubation of HepG2 cells at 20°C to block the formation of vesicles from the Golgi (Griffiths et al., 1985) increased membrane binding of syndapin II (Fig. 6A). This finding might suggest a role of syndapin II in the formation of vesicles from the Golgi. To provide further evidence for an association of syndapin II with the Golgi complex, we studied the localization of syndapin II in COS-7 cells. Untransfected cells labeled with a syndapin II-specific antibody (P339) (Qualmann and Kelly, 2000) showed a very weak staining that reflected the generally low expression levels of syndapin II isoforms. Immunostaining was detectable in the cytoplasm and in circular structures adjacent to the nuclei (Fig. 6B,E). Cells transfected with Xpress-tagged syndapin II-l showed signals of varying intensity but were often also marked by perinuclear syndapin II accumulations (Fig. 6B and short exposure insert in 6B).

Immunostaining for syntaxin 6, a SNARE protein residing in the membranes of the TGN (Bock et al., 1997), led to signals confined to perinuclear sites, which also often appeared circular (Fig. 6C,F). Superimposition of the syndapin II and syntaxin 6 staining revealed a co-localization of both proteins at the TGN (Fig. 6D,G), which is especially well seen at high magnification (Fig. 6E-G). In addition, a co-localization of syndapin II and TGN38, another marker of the TGN, was observed in HeLa cells (J.D. and P.W., unpublished).

To prove that the observed co-localization of syndapin II and syntaxin 6 indeed reflects localization to the TGN, the cells were incubated with brefeldin A (BFA). BFA treatment leads to fusion of the Golgi complex with the ER and to a collapse of the TGN. Many cells treated with BFA displayed an intense syntaxin 6 staining that was condensed to small areas adjacent to the nucleus (Fig. 6I,L). Other cells completely lacked a perinuclear-accumulated signal but instead showed a weak and dispersed labeling. Similar effects were observed with anti-TGN38 antibodies (not shown). No labeling of endogenous (Fig. 6H) or overexpressed syndapin II (Fig. 6K) was present at sites of condensed syntaxin 6 staining, as clearly shown in merged images (Fig. 6J,M), but a dispersed syndapin distribution was observed. Thus, the syndapin II co-localization with integral TGN proteins was abolished in cells lacking a functional TGN.

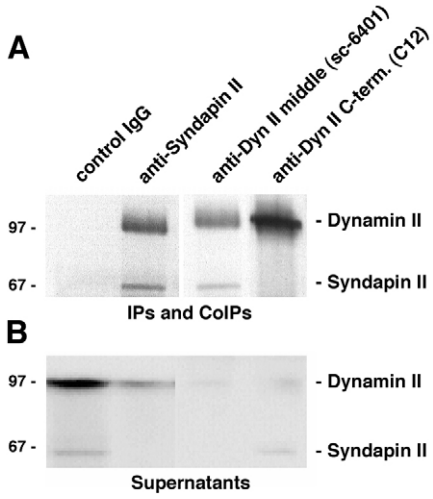

Fig. 4. Dynamin II and syndapin II interact in vivo. (A) Complexes of dynamin II with syndapin II were immunoprecipitated from HepG2 cell extracts using anti-syndapin II antibodies (3685) and the anti-dynamin (Dyn) II antibody sc-6401, which recognizes an internal sequence of dynamin II, respectively. Eluates were analyzed by immunoblotting using the antibodies 3685 (anti-syndapin II) and C12 (anti-dynamin II). The antibody C12, which specifically recognizes the C-terminus of dynamin II, only immunoprecipitated dynamin II, but did not co-immunoprecipitate syndapin II. (B) The supernatants of the immunoprecipitations were precipitated with methanol and then immunoblotted with anti-dynamin II and anti-syndapin II antibodies. IPs, immunoprecipitates; CoIPs, co-immunoprecipitates.

Syndapin II protein complexes have a crucial role in formation of transport vesicles from Golgi membranes in vitro

Previous studies have provided evidence for an essential function of dynamin II in the formation of transport vesicles at Golgi membranes (Jones et al., 1998; J. Dong, PhD thesis). Our biochemical, immunocytochemical and cell biological data

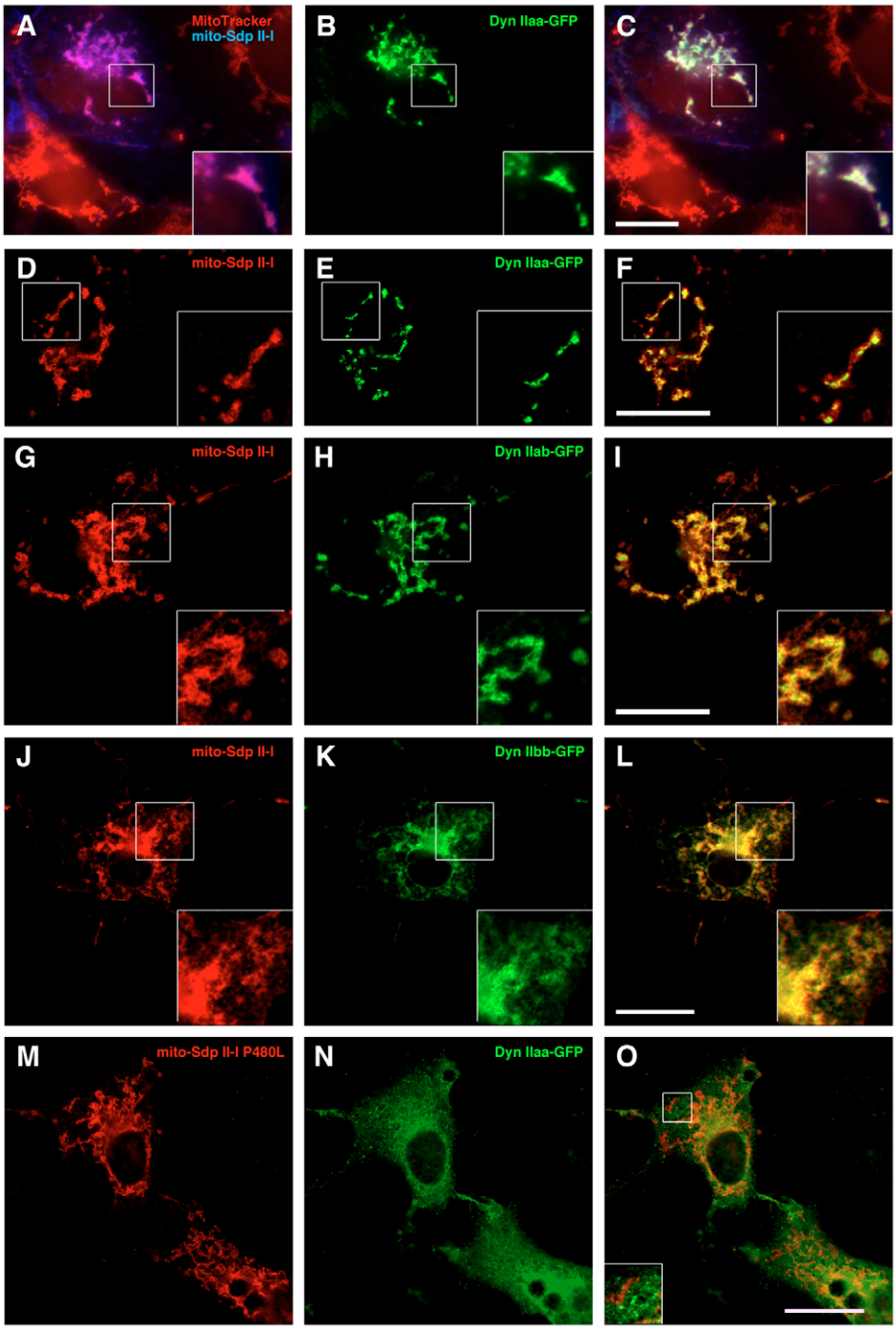

Fig. 5. Reconstitution of complexes of syndapin II with dynamin II at cellular membranes in vivo. (A-L) Mitochondrially targeted full-length syndapin II-l, detected by anti-Flag immunostaining (A,D,G,J), recruits different GFP-tagged splice variants of dynamin II (B,E,H,K) when cotransfected in COS-7 cells, as also demonstrated by merging the fluorescence channels (C,F,I,L). (A-F) Recruitment of dynamin IIaa-GFP (B,E) by mito-syndapin II-l that, in A, was additionally co-localized with MitoTracker (in blue; merge in A thus appears magenta). (G-I) In vivo reconstitution of protein complexes composed of mito-syndapin II-l and dynamin IIab-GFP. (J-L) Mito-syndapin II-l efficiently recruits dynamin IIbb-GFP. (M-O) By contrast, in cells cotransfected with mito-syndapin II-l P480L (M), no such recruitment was observable, but dynamin IIaa-GFP (N) shows a rather diffuse localization. O represents the corresponding merged image. Insets are twofold enlargements of boxed areas. Dyn, dynamin; mito-Sdp, mito-syndapin. Bars, 15 μm.

suggest that this function might involve syndapin II. To examine whether syndapins are crucial for this process and, specifically, whether interactions of the syndapin SH3 domain with dynamin II are required, we used an experimental system invented by Tooze and Huttner that allows the reconstitution, measurement and manipulation of the budding of vesicles from isolated Golgi membranes in vitro (Tooze and Huttner, 1992; Westermann et al., 1996; Dong et al., 2000b). The assay has been extensively characterized (Westermann et al., 1996; Dong et al., 2000b) and is based on the incubation of cell extracts with ATP, GTP, an ATP-regenerating system and the subsequent isolation of newly formed vesicles by differential centrifugation. Newly synthesized, mature proteins were labeled and accumulated in the TGN according to Griffiths et al. (Griffiths et al., 1985) by labeling of HepG2 cells with [^{35}S]methionine at 37°C and subsequent incubation at 20°C in the presence of excess unlabeled methionine. Transport vesicles formed were isolated by differential centrifugation and vesicle-bound radioactivity was determined. Under standard assay conditions, about 30% of labeled luminal proteins are packed into transport vesicles. To compare packaging ratios of different experiments, the corresponding standard values of each experiment were arbitrarily set to 100. In a first set of experiments, we addressed the potential role of syndapin-

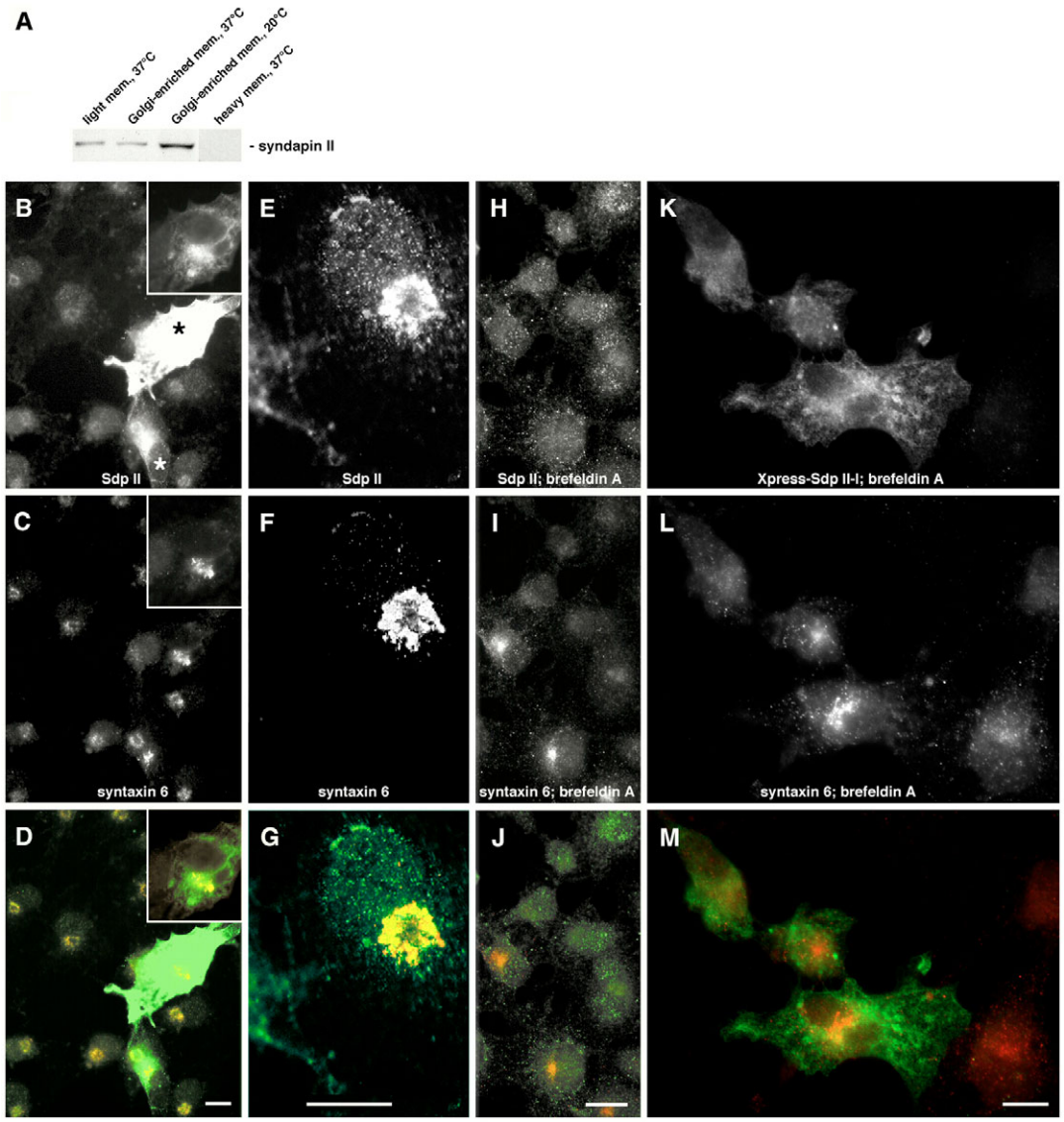

Fig. 6. Syndapin II is bound to Golgi-enriched membranes of HepG2 cells and can be localized to the Golgi complex of COS-7 cells by immunofluorescence analysis. (A) After incubation of HepG2 cells at 37°C or at 20°C (Golgi exit block), syndapin II is detected in light membranes (mem.) and in Golgi-enriched membranes but not in heavy membranes sedimenting through 1.2 M sucrose. 30 μg membrane proteins were separated by SDS-PAGE, blotted and analyzed with anti-syndapin II antibody 3685. (B-J) Syndapin II (Sdp II) co-localizes with the Golgi marker syntaxin 6 in both untransfected COS-7 cells and in cells transfected with syndapin II-l, as seen well in the merged images (D-J; syndapin II in green, syntaxin 6 in red). Syndapin II was detected by the syndapin II-specific antibody P339 (B,E,H) and syntaxin 6 was detected with a monoclonal anti-syntaxin 6 antibody (C,F,I). Similar to endogenous syndapin II, overexpressed Xpress-tagged syndapin II-l also shows a perinuclear co-localization with syntaxin 6 (B-D). The two cells expressing Xpress-tagged syndapin II-l shown in B are marked by asterisks. Inserts show a shorter exposure of perinuclear region of the upper transfected cell. (E-G) High magnifications show that endogenous syndapin II (E) co-localizes very well with syntaxin 6 (F). (H-M) After incubation of COS-7 cells with brefeldin A to disrupt the TGN, syntaxin 6 immunostaining was found either to be collapsed into small perinuclear dots or to be dispersed (I,L). The immunostaining of endogenous (H) and overexpressed syndapin II (K) was mainly dispersed and showed no co-localization with the perinuclear syntaxin 6 accumulations formed upon BFA treatment (J,M). Bars, 10 μm.

dynamin complexes by adding purified recombinant GST-syndapin SH3 domain to the cytosol, which is required for the reconstitution of vesicle formation. We observed that the addition of GST-syndapin II SH3 inhibited vesicle formation from Golgi membranes in a dose-dependent manner (Fig. 7A, circles). The impact of another dynamin-binding SH3 domain, that of amphiphysin, was significantly weaker than that of the syndapin II SH3 domain (Fig. 7A, squares). However, both SH3 domains had clear and dose-dependent inhibitory effects on vesicle formation (Fig. 7A). Since the addition of GST alone was not inhibitory (data not shown), the inhibitory effect of the SH3 domains was specific.

To examine the functional importance of syndapin II for vesicle formation, we added an anti-syndapin II antiserum to the cytosol required for supporting the Golgi budding assays (Fig. 7B). The antiserum is highly specific for the syndapin II

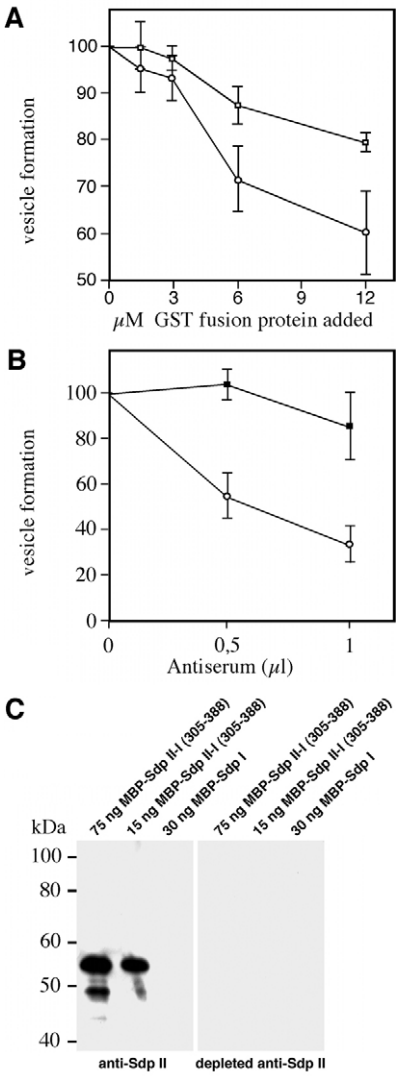

Fig. 7. Complex formation between syndapin II and dynamin II is required for vesicle formation from isolated Golgi membranes. (A) Vesicle formation from Golgi-enriched membranes of HepG2 cells is inhibited in a dose-dependent manner by the addition of the GST-tagged SH3 domain of the dynamin II-binding proteins syndapin II (circles) and amphiphysin II (squares). The assay contained Golgi-enriched membranes, ATP, GTP and 40 μg cytosolic proteins as described in the Materials and Methods. Vesicles formed were sedimented and the radioactivity of newly synthesized proteins that were packed into the vesicles was determined. The value obtained under standard conditions is arbitrarily set to 100. The experiments shown were performed in triplicate and s.d. are given. (B) The anti-syndapin II antiserum 3685 inhibits vesicle formation at Golgi-enriched membranes in a dose-dependent manner (open circles). When syndapin-specific antibodies were depleted from the antiserum 3685, inhibition was markedly reduced (filled squares). (C) Specificities and affinities of the original (left) and the depleted antiserum 3685 (right) are shown by immunostaining of western blots with 75 ng (lanes 1,4) and 15 ng (lanes 2,5) MBP-syndapin II antigen [MBP-Sdp II-I (305-388)] as well as with 30 ng (lanes 3,6) MBP-full-length syndapin I (MBP-Sdp I).

isoform and does not recognize syndapin I (Fig. 7C), and was found to inhibit vesicle formation (Fig. 7B, circles). This inhibition of vesicle formation was again strongly dose dependent (Fig. 7B, circles). As a control, we depleted the antiserum for anti-syndapin II antibodies by consecutive pre-incubations with two immobilized syndapin fusion proteins. After such pre-incubations, the serum no longer contained any anti-syndapin II antibodies (Fig. 7C) and was no longer able to interfere with vesicle formation (Fig. 7B; filled squares). Thus, the anti-syndapin II antibodies that were removed were responsible for the inhibition.

The interaction of the syndapin II SH3 domain with the dynamin II PRD is important for vesicle formation from the TGN in vivo

To prove that our detailed mechanistical analyses in vitro reflect the situation in vivo, we followed the trafficking of TGN-derived vesicles to the plasma membrane by labeling them with a temperature-sensitive vesicular stomatitis virus glycoprotein (VSVG)-GFP, according to Cao et al. (Cao et al., 2000) and asked whether interfering with the interaction between syndapin II and dynamin II by different means would inhibit membrane trafficking from the TGN. In control cells transfected with VSVG-GFP alone, VSVG-GFP accumulated in the ER at 40°C, as previously described by Presley et al. (Presley et al., 1997). Upon shifting the cells to 32°C, VSVG underwent ER-to-Golgi transport within minutes. The time point of 15 minutes thus served as a start for our Golgi-to-PM chase. After this time, the ER staining was strongly reduced and VSVG-GFP was strongly accumulated in a perinuclear spot representing the Golgi (Fig. 8A). After 45 minutes at 32°C, the VSVG fluorescence was somewhat decreased in the Golgi area and started to appear within the periphery of cells transfected with VSVG-GFP (not shown). After 90 minutes, the cells showed a relatively continuous plasma membrane localization of VSVG-GFP and, correspondingly, fluorescence within the Golgi area was markedly reduced (Fig. 8B).

By contrast, when we cotransfected the cells with a plasmid encoding a dynamin II variant incapable of associating with syndapin II (dynamin IIΔPRD; Fig. 2A), after 90 minutes the cells still largely displayed a situation very similar to the 15 minutes time point of the VSVG-GFP chase (Fig. 8C,D). VSVG-GFP was still strongly accumulated in the Golgi area and had not been transported effectively to the plasma membrane, suggesting an inhibition of TGN exit. Careful quantitative evaluations of the TGN-to-PM transport, which were essentially performed as described by Cao et al. (Cao et al., 2000), clearly showed that cells double transfected with dynamin IIΔPRD showed no reduction of averaged fluorescence signal within the region of interest during the 90 minutes chase (Fig. 8I). By contrast, examinations of VSVG-transfected control cells showed the expected significant reduction in fluorescence signal in the Golgi area after 90 minutes at 32°C (Fig. 8I).

Similar to interfering with interactions between dynamin II and syndapin II by overexpressing dynamin IIΔPRD, co-expression of the syndapin II SH3 domain had a marked inhibitory effect on Golgi-to-PM transport as well. The VSVG-GFP signal remained strongly accumulated in the perinuclear area in cells overexpressing the isolated dynamin-binding SH3 domain of syndapin II (Fig. 8F). Quantitative measurements demonstrated that there was no reduction of VSVG-GFP signal intensity in the perinuclear area of interest after 90 minutes compared with the start value (Fig. 8I).

Journal of Cell Science

Journal of Cell Science

Overexpression of full-length syndapin II-l, by contrast, had no inhibitory effect. After 90 minutes, cells overexpressing syndapin II-l displayed VSVG-GFP at the plasma membrane (Fig. 8H). Our quantitative evaluations confirmed the effective transport from the TGN towards the plasma membrane, as the fluorescence intensities in the perinuclear area measured at 90 minutes at 32°C were even lower than those in VSVG-GFP control cells (Fig. 8I). Quantitative examinations of an intermediate time point (45 minutes at 32°C) also showed that cells overexpressing syndapin II-l tend to transport VSVG-GFP out of the Golgi more effectively than do control cells (63.2±24.3% compared with 89.0±0.6%).

In summary, our quantitative functional studies demonstrate that interfering with interactions between dynamin II and syndapin II in living cells causes an inhibition of TGN exit, whereas increased syndapin II levels do not inhibit but instead cause some increase in Golgi-to-PM transport.

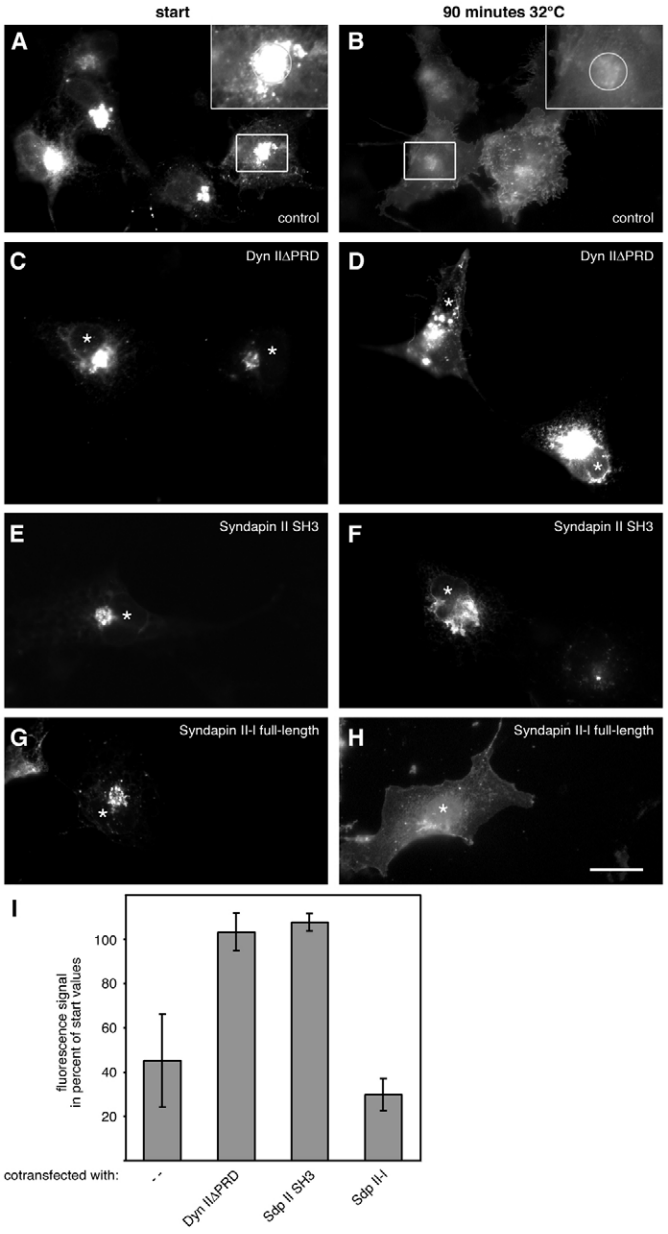

Syndapin II is a crucial component in TGN exit

Our in vitro reconstitutions strongly suggested that syndapin II is a crucial component of vesicle formation from Golgi membranes (Fig. 7). Furthermore, both our in vitro and our in vivo examinations demonstrated that SH3 domain interactions are explicitly involved (Figs 7 and 8). To test a putative dependency of vesicle formation from the TGN on syndapin II in vivo, we acutely interfered with syndapin functions by introducing anti-syndapin antibodies into cells expressing VSVG-GFP using the BioPorter method (Fig. 9). Introduction of anti-syndapin antibodies led to a potent block in TGN exit, as cells still displayed a perinuclear accumulation of the VSVG-GFP signal after 90 minutes at 32°C (Fig. 9D) that was similar to the distribution at the start time point (Fig. 9C). This inhibition is specifically a result of the anti-syndapin reagent introduced, as demonstrated by examining cells that were only treated with BioPorter alone or with anti-syndapin preimmune. In both cases, normal VSVG-GFP transport to the plasma membrane was observed, i.e. the cells displayed VSVG-GFP at the plasma membrane after 90 minutes at 32°C (data not shown and Fig. 9B, respectively). Quantitative measurements of the VSVG-GFP fluorescence in the perinuclear region of interest clearly confirmed the undisturbed transport in cells treated either with BioPorter or BioPorter plus anti-syndapin preimmune. By contrast, the almost unchanged VSVG-GFP fluorescence intensity in the Golgi area demonstrates the prominent inhibition of TGN exit upon introduction of anti-syndapin antibodies (Fig. 9E). Similar to the effects observed upon overexpression of dynamin IIΔPRD and of the syndapin II SH3 domain, VSVG-GFP largely remained arrested in the Golgi in cells in which syndapin II functions were disturbed by anti-syndapin antibodies.

Fig. 8. Trafficking of VSVG-GFP from the Golgi to the plasma membrane is inhibited upon interfering with interactions between dynamin II and syndapin II. (A,B) COS-7 cells transfected with a temperature-sensitive VSVG-GFP showed a strong perinuclear fluorescence after 15 minutes at 32°C (A; start of chase), which declined as fluorescent material was transported to the plasma membrane after 90 minutes at 32°C (B). Magnifications of boxed areas in A and B display the region of interest (gray circle) used for the quantitative image analyses (I). (C,D) Cells co-overexpressing Myc-tagged dynamin IIΔPRD (Dyn IIΔPRD) displayed perinuclear accumulations of VSVG-GFP at the start of chase (C) and after 90 minutes at 32°C (D). (E,F) Cells overexpressing the Xpress-tagged syndapin II SH3 domain also show an arrest of VSVG-GFP in the perinuclear region (F). (G,H) By contrast, co-overexpression of full-length syndapin II-l had no negative effect on Golgi-to-PM transport but VSVG-GFP was observed at the plasma membrane after 90 minutes (H). Images were processed by Adobe Photoshop to visualize clearly the different VSVG-GFP distributions. Co-transfected cells are marked by asterisks. Bar, 20 μm. (I) Averaged fluorescence intensities within the perinuclear region of interest after 90 minutes at 32°C expressed as percentage of start values. Fluorescence was measured as 8-bit gray values by unbiased experimenters. 255 corresponds to white, 0 to black. Background values were subtracted. Control (- -): start of chase, 275 cells; 90 minutes, 280 cells. Dynamin (Dyn) IIΔPRD: start, 83 cells; 90 minutes, 82 cells. Syndapin II SH3 domain (Sdp II SH3): start, 57 cells; 90 minutes, 32 cells. Syndapin II-l full-length (Sdp II-I): start, 66 cells; 90 minutes, 52 cells. Error bars represent standard deviations between independent data sets.

Syndapin-dynamin complexes promote vesicle formation

Dynamin II and syndapin II, and their ability to undergo SH3 domain and PRD interactions, are important for vesicle formation at the TGN. We therefore directly addressed whether it would be possible to reconstitute vesicle formation with a cytosolic fraction containing complexes of syndapin II and dynamin II, instead of the full cytosol prepared from HepG2 cells. For this purpose, we performed a glycerol gradient fractionation of the cytosol and selected fraction 6 corresponding to about 160-230 kDa (compare Fig. 1). This fraction should contain neither monomeric dynamin nor syndapin but instead should contain complexes of syndapin II with dynamin II. To prove that syndapin II and dynamin II not only co-fractionate in this fraction but also exist in a complex with each other, we performed additional immunoprecipitation analyses with material from fraction 6. Fig. 10A shows that, similar to the co-immunoprecipitations from HepG2 cell extracts (Fig. 4), anti-syndapin II antibodies immunoprecipitate syndapin-dynamin complexes from gradient fraction 6. When we added aliquots of fraction 6 to our in vitro budding assay, it was sufficient to stimulate vesicle formation to about 60% of standard assays (Fig. 10, circles), i.e. the assay became independent of the presence of full cytosol. Importantly, after immunoprecipitation of the syndapin-dynamin complex, the remaining proteins of fraction 6 were almost unable to support vesicle formation (Fig. 10, squares). Since co-immunoprecipitations with anti-syndapin antibodies failed to deplete the dynamin pool, similar to the immunoprecipitation analysis from HepG2 cell extracts shown previously (Fig. 4), these results furthermore suggest that dynamin II alone is not sufficient to promote vesicle formation under the conditions of the assay. The lack of vesicle formation under these conditions also firmly rules out that artificial Golgi fragmentations, which could theoretically falsify the results, occur in the assay. Membrane fragmentations had been observed upon addition of high amounts of recombinant, purified dynamin I to membranes in vitro (Sweitzer and Hinshaw, 1998). Our observations are in line with the previously reported extensive characterization of the assay,

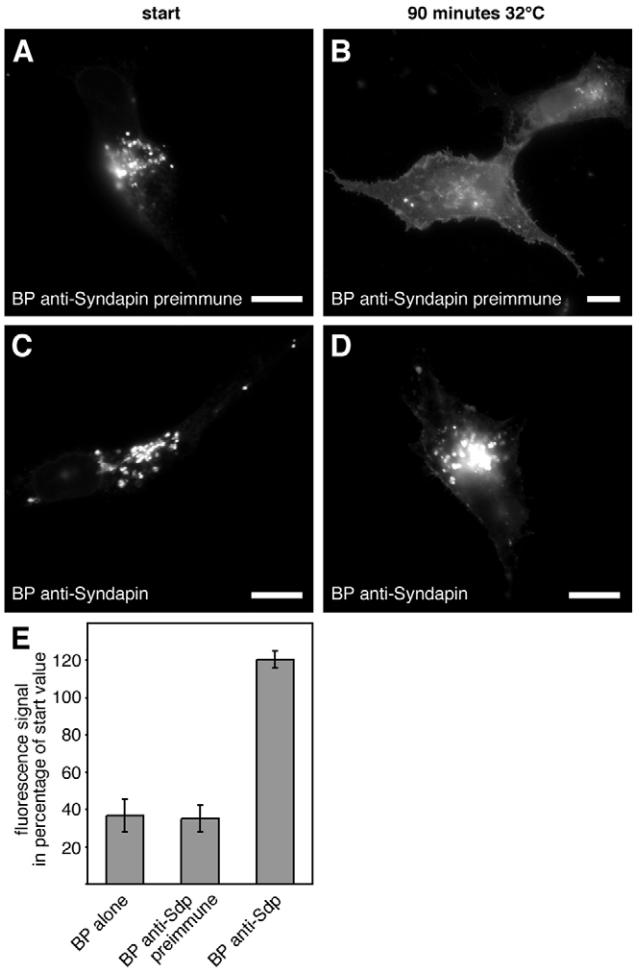

Fig. 9. Acute interference with syndapin functions by introducing anti-syndapin antibodies blocks Golgi-to-PM transport of VSVG-GFP. (A,B) VSVG-GFP accumulated in the Golgi at the start of chase (A) and reached the plasma membrane after 90 minutes (end of chase) in cells treated with BioPorter (BP) and anti-syndapin preimmune (B). (C,D) By contrast, cells treated with BioPorter and anti-syndapin immunoreagent showed an arrest of VSVG-GFP signal in the perinuclear area. Images were processed by Adobe Photoshop to visualize clearly the different VSVG-GFP distributions. Bars, 10 μm. (E) Quantitative analyses of fluorescence signals in the perinuclear regions of interest clearly show the undisturbed Golgi-to-PM trafficking in cells treated with BioPorter (BP alone) or BioPorter plus anti-syndapin preimmune (BP anti-Sdp preimmune), and the inhibition of Golgi exit of VSVG-GFP in cells into which anti-syndapin antibodies (BP anti-Sdp) had been introduced. Error bars represent standard deviations between independent data sets.

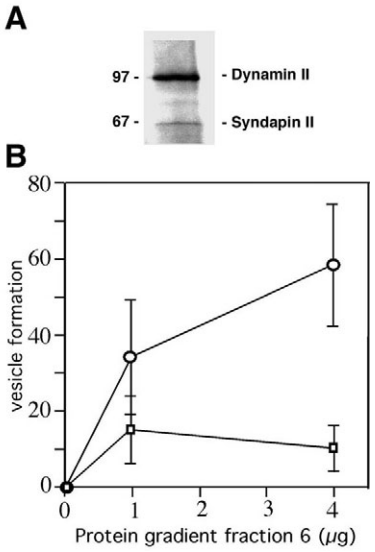

Fig. 10. The complex of dynamin II and syndapin II promotes vesicle formation at Golgi-enriched membranes in vitro. The protein fraction 6 (obtained by fractionation of cytosolic proteins of HepG2 cells on a glycerol gradient) that contains complexes of dynamin II with syndapin II, as demonstrated by co-immunoprecipitation with anti-syndapin II antibodies (3685) and immunoblotting with anti-syndapin II and anti-dynamin II antibodies (A), is sufficient for promoting vesicle formation at Golgi-enriched membranes in vitro (B, circles). The stimulatory activity can be removed from fraction 6 by immunoprecipitation with anti-syndapin II antibodies (B, squares).

Journal of Cell Science

which for example showed the absence of GM130, a resident Golgi protein, from the obtained vesicle fractions (Westermann et al., 2000).

Taken together, our examinations show that: (1) syndapin II forms functional complexes with the variants of the GTPase dynamin II in vitro and in vivo; (2) such complexes are capable and necessary to promote budding from TGN membranes; and (3) any interference with the assembly of syndapin-dynamin complexes consistently inhibits vesicle formation, as demonstarted by the inhibitory effects caused by an excess of the syndapin SH3 domain or of a dynamin II lacking the syndapin-binding interface, as well as by the block of vesicle formation caused by applying anti-syndapin antibodies.

Discussion

It is commonly accepted that GTPases of the dynamin protein family are crucial for the formation of clathrin-coated vesicles at the plasma membrane. However, whereas it is well studied that similar clathrin coat structures also support the formation of vesicles from the TGN, the role of dynamins in vesicle formation from these donor membranes remains controversial (reviewed by Hinshaw, 2000; McNiven et al., 2000; Sever et al., 2000). An experimental route to clarify this and to gain knowledge about the molecular mechanisms of Golgi vesicle formation is to examine Golgi trafficking pathways for the functional involvement of dynamins and accessory proteins, which seem to work in close conjunction with dynamin in the better understood process of endocytic vesicle formation.

Here, we show that syndapin II interacts with dynamin II, as demonstrated by co-precipitation experiments, by co-immunoprecipitations of the endogenous proteins from HepG2 cell extracts using either syndapin II- or dynamin II-specific antibodies and by in vivo reconstitutions. The latter analyses exclude the theoretical possibility of post-homogenization artifacts. The association of syndapin II and dynamin II depends on the SH3 domain of syndapin II and the PRD of dynamin II and is direct, as revealed by our in vitro binding studies. These data are strongly supported by the observations that a syndapin II with a mutated SH3 domain failed to recruit dynamin II in vivo and that the antibody C12, which interacts with the PRD of dynamin II, failed to co-immunopreciptate syndapin II.

Our further analyses strongly suggest that complexes of syndapin II with dynamin II are involved in vesicle formation from the Golgi complex. Syndapin II was localized to Golgi membranes in both biochemical analyses, as well as in immunofluorescence studies together with syntaxin 6. Also, the co-localization of epitope-tagged syndapin II-l with dynamin IIaa-GFP, which was demonstrated to accumulate at the Golgi complex (Cao et al., 1998), supports the Golgi localization of syndapin II. Consistently, the syndapin II localization was affected by BFA treatment. We therefore conclude that the perinuclear localization of syndapin II indeed represents the Golgi complex and, furthermore, that association of syndapin II with the Golgi depends on a functional Golgi complex.

Dynamin II was described as associating with both the plasma membrane and the Golgi complex and it was shown to promote the formation of Golgi-derived transport vesicles in in vitro assays (Jones et al., 1998; J. Dong, PhD thesis). Also, in vivo studies suggest that dynamin II is somehow involved in vesicle formation from the Golgi (Cao et al., 2000; Yang et al., 2001). Our studies clearly suggest that the role of dynamin II in vesicle formation at the Golgi relies on complex formation with syndapin II. A function for syndapin II in vesicle formation is in line with the observed syndapin II accumulation at Golgi membranes upon inhibition of vesicle formation by a 20°C block. In vitro reconstitutions of vesicle formation from Golgi membranes allowed us to prove the importance of syndapin II and dynamin II, and to reveal mechanistical details of the process. Vesicle formation was inhibited by anti-syndapin II antibodies added to the HepG2 cell extracts required for supporting the vesicle formation process. The pool of dynamin II not in complex with syndapin II, and thus not affected by anti-syndapin antibodies, was obviously not able to support vesicle formation. Similar results were obtained in vivo: introduction of anti-syndapin antibodies into living cells strongly impaired the TGN exit of VSVG-GFP, suggesting that syndapins are crucial components of Golgi vesicle formation. This conclusion is reminiscent of the importance of syndapins in the dynamin-dependent formation of endocytic vesicles (Braun et al., 2005).

Our analyses also clearly demonstrate that, in particular, the interaction of syndapin II and dynamin II is of importance. Addition of the dynamin-binding syndapin II SH3 domain had a strong inhibitory and dose-dependent effect in the in vitro reconstitutions of vesicle formation. Consistently, overexpression of the syndapin II SH3 domain caused a strong arrest of vesicle formation from the TGN in vivo. These data are in line with the SH3 domain of syndapin II acting as a dominant-negative tool in dynamin-dependent vesicle formation from the plasma membrane (Qualmann and Kelly, 2000). Also consistent with the model that interactions of the dynamin PRD with syndapins are important for vesicle formation in Golgi-to-PM transport are the findings that: (1) an excess PRD of dynamin II inhibits vesicle formation in vitro (Dong et al., 2000b); and (2) overexpression of dynamin IIΔPRD, i.e. of a dynamin lacking the syndapin-binding interface, had a significant negative impact on Golgi vesicle formation in vivo, as shown by a failure of VSVG-GFP to traffic from the Golgi to the plasma membrane. A recently published study (Bonazzi et al., 2005) failed to find any inhibition of Golgi-to-PM transport of VSVG-GFP using a different dynamin-derived tool, dynamin II K44A, applying a different technique of analysis and only covering early time points. The apparent contradiction may thus merely reflect a lack of comparability. Other studies are very well in line with the kinetics of VSVG-GFP trafficking we observed (Presley et al., 1997; Cao et al., 2005), as well as with our observation that dynamin IIΔPRD causes a disruption of Golgi-to-PM transport (Cao et al., 2005). Cao et al. (Cao et al., 2005) suggested that the inhibition might be a result of the binding of cortactin to the PRD of dynamin II. It is known that several so-called accessory SH3-domain-containing proteins bind to different molecular interfaces within the extended PRD of dynamins (Grabs et al., 1997). The proline-rich sequence recognized by the syndapin SH3 domain seems to be very different from that bound by the cortactin SH3 domain (our unpublished results). This opens the exciting possibility that – very similar to the endocytic process – several of these factors bind simultaneously to dynamins. In addition, our fractionation and co-immunoprecipitation analyses clearly show that complexes

Journal of Cell Science

of syndapin II with dynamin II represent a sub-pool of the dynamin present in the cell. Thus, a sequential and independent complex formation of cortactin and syndapin with dynamin II is also plausible and it will therefore be exciting to unravel the detailed molecular mechanisms that underlie the orchestrated action of the different dynamin-binding proteins in vesicle formation processes.

Our current study conclusively demonstrates that syndapin II, as well as syndapin-dynamin complex formation, are important for vesicle formation from the Golgi in vivo. Importantly, our in vitro reconstitutions also strongly suggest that complexes containing syndapin II and dynamin II are not only crucial but are also sufficient for vesicle formation from Golgi membranes and may thus represent a minimal machinery supporting vesicle formation.

The involvement of complexes of syndapin II with dynamin II in Golgi vesicle formation appears reminiscent of mechanisms of endocytic vesicle formation. Syndapin I was demonstrated to associate strongly with dynamin I both in vitro and in vivo, and disrupting syndapin interactions through an excess of the dynamin-binding SH3 domain inhibited vesicle formation both in vivo (Qualmann and Kelly, 2000) and in in vitro reconstitution experiments (Simpson et al., 1999). Consistently, impairing syndapin functions by the introduction of anti-syndapin antibodies disturbed the receptor-mediated endocytosis of transferrin (Braun et al., 2005). Since syndapins control the activity of the Arp2/3 actin polymerization machinery (Qualmann et al., 1999; Qualmann and Kelly, 2000), and since such cytoskeletal interactions appear to be of importance for endocytosis (Kessels and Qualmann, 2002), syndapins might act as molecular links between the cortical actin cytoskeleton and the endocytic machinery (Kessels and Qualmann, 2004) and might help to integrate cytoskeletal functions into the vesicle formation process (Qualmann et al., 2000; Kessels and Qualmann, 2002). It seems possible that syndapins might also link cytoskeletal functions to vesicle formation originating from the Golgi. Similar to the plasma membrane, Golgi membranes are also associated with a specialized cytoskeleton comprising actin and spectrin (reviewed by Beck and Nelson, 1998; De Matteis and Morrow, 2000; Stamnes, 2002) that seems to support membrane topology and organelle organization (di Campli et al., 1999; Valderrama et al., 1998). By analogy to the cortical cytoskeleton (Qualmann and Kessels, 2002), Golgi-associated cytoskeletal structures appear to be involved in supporting membrane trafficking processes (Fucini et al., 2002; Müsch et al., 2001; Valderrama et al., 2001; Cao et al., 2005).

In summary, our biochemical, immunocytochemical and cell biological examinations provide conclusive evidence for an association of syndapin II with dynamin II and with the TGN, and for a complex of syndapin II and dynamin II being an essential component of the budding machinery at Golgi membranes. Consistently, any interference with the interaction between syndapin II and dynamin II disrupts vesicle formation in vitro and in vivo. Considering the fact that syndapins and dynamins also have a role in endocytosis and that the molecular details resemble those revealed for syndapin-dynamin function in Golgi vesicle formation in this study, it seems likely that the similarity of the basic mechanisms of vesicle budding at the plasma membrane and at the Golgi complex extends to the roles of the so-called accessory dynamin-binding proteins.

Materials and Methods

Antibodies

The anti-dynamin II PRD antibody C12 was raised in rabbits and affinity purified (Maier et al., 1996). Antibody sc-6401, which is specific for the dynamin II N-terminus, was from Santa Cruz Biotechnology. The syndapin II-specific antibodies 3685 (rabbit), 2521 (rabbit) and P339 (guinea-pig), as well as rabbit anti-GST antibodies, were described previously (Qualmann and Kelly, 2000; Qualmann et al., 1999). Anti-syntaxin 6 antibodies were from Transduction Laboratories; monoclonal anti-Flag (M2) and anti-GFP antibodies (B34) were from Sigma and Babco, respectively.

Serum 3685 was depleted for syndapin II-specific antibodies by double affinity purification using a fusion protein of maltose-binding protein (MBP) and syndapin II (aa 305-388) bound to nitrocellulose, and subsequently using a GST-syndapin II (aa 305-388) fusion protein bound to ACTIGEL (Sterogene Bioseparations).

Plasmids and expression of protein constructs

Expression and purification of S-peptide-tagged dynamin II pleckstrin-homology domain (S-Dyn II PH domain) and PRD (S-Dyn II PRD) in *Escherichia coli* were described previously (Dong et al., 2000a). Dynamin IIaa-GFP and dynamin IIab-GFP plasmids were obtained from M. McNiven (Mayo Clinic and Foundation, Rochester, MN). Dynamin IIbb was generated by PCR and subcloned into pEGFP-N1. To generate dynamin IIaaΔPRD-GFP (aa 1-746), the cDNA of rat dynamin IIaa was cut at an internal *Sca*I site and fused to an appropriate PCR fragment. Dynamin IIaaΔPRD was subcloned into the *Hin*dIII and *Eco*RI sites of pcDNA3.1/Myc-His (Invitrogen) to generate dynamin IIaaΔPRD-Myc. Plasmids encoding Xpress-tagged syndapin II-l, Xpress-tagged syndapin II SH3 domain, mitochondria-targeted full-length syndapin II-l and syndapin II-l P480L were described previously (Qualmann and Kelly, 2000; Kessels and Qualmann, 2002). Flag-tagged syndapin II-l was generated by subcloning into pCMV-Tag2B (Stratagene). GST fusion proteins of syndapin II and of its SH3 domain, as well as MBP fusion proteins of syndapins and fragments thereof, were expressed in *E. coli* and purified as described (Qualmann and Kelly, 2000).

Co-precipitation assays

HEK293 cells were transfected with different GFP-tagged constructs using LipofectAMINE PLUS reagent (Invitrogen), harvested and lysed in IP buffer (10 mM HEPES, 1 mM EGTA, 0.1 mM $MgCl_2$, 100 mM NaCl, 1% Triton X-100, pH 7.4). High-speed supernatants prepared from the lysates were incubated with immobilized GST-syndapin II SH3 domain or GST alone at 4°C for 16 hours. Precipitated protein complexes were analyzed by SDS-PAGE and immunoblotted with anti-GFP antibodies.

For affinity purifications with S-Dyn II PRD or S-Dyn II PH domain, 10 μg protein were immobilized to S-protein agarose and incubated with HepG2 and HEK293 cell lysates, respectively, containing 1-2 mg protein in buffer B [20 mM HEPES, pH 7.2, 150 mM NaCl, 0.1% Triton X-100, supplemented with protease inhibitor mixture (PI; Roche)] at 4°C for 2 hours. After washing with buffer B, bound proteins were extracted with SDS sample buffer and analyzed by immunoblotting with anti-syndapin II antibodies.

Glycerol gradient centrifugation of HepG2 cytosolic proteins

HepG2 cells were collected and disrupted in 100 mM NaCl, 20 mM HEPES, pH 7.2, 1 mM dithiothreitol, 2 mM $MgCl_2$, supplemented with PI mixture using a ball-bearing homogenizer. After centrifugation for 10 minutes at 1000 ***g***, the post-nuclear supernatant was centrifuged for 30 minutes at 100,000 ***g***. Cytosolic proteins were concentrated fivefold in a dialysis bag coated with dry Sephadex G200 and dialyzed against 10 mM HEPES, pH 7.2, 1 mM $MgCl_2$, 1 mM EDTA, 50 mM potassium acetate. Protein samples (0.5 ml) were run on a 10-30% glycerol gradient for 17 hours at 190,000 ***g*** (43,000 rpm Beckman) using a SW60 rotor. Gradients were divided into 11 fractions. Proteins within the individual fractions were analyzed by immunoblotting.

In vitro reconstitution of the interaction between syndapin SH3 domain and dynamin PRD

For reconstitution of interactions between the syndapin SH3 domain and the dynamin II PRD domain, 5 μg S-Dyn II PRD was bound to 50 μl S-protein agarose. 5 μg S-Dyn II PH domain was used as control. After washing, 10 μg GST-syndapin II SH3 domain was added in buffer A (20 mM HEPES, pH 7.2, 50 mM NaCl, 0.1% Triton X-100, PI) and incubated for 1 hour at 4°C. After washing with buffer A, bound proteins were extracted with SDS sample buffer and analyzed by SDS-PAGE and Coomassie Brilliant Blue staining.

Immunoprecipitations

Lysates of HepG2 cells grown on dishes coated with S-collagen or of transfected HEK293 cells were incubated in buffer C (20 mM HEPES, pH 7.2, 150 mM NaCl, 1% Triton X-100, PI) for 30 minutes on ice. After centrifugation for 10 minutes at 100,000 ***g***, the supernatant (500 μl) was incubated with 3 μg antibody at 4°C for 1-2 hours. 50 μl of protein A-agarose and protein G-agarose was added to rabbit

Journal of Cell Science

or mouse IgGs and goat IgGs, respectively. After a further 2 hours of incubation and extensive washing with 150 mM NaCl, 1% Triton X-100, 50 mM Tris-HCl, pH 7.5, bound proteins were eluted with SDS sample buffer and immunoblotted using anti-syndapin II and anti-dynamin II antibodies.

The HepG2 cell cytosol fraction and glycerol gradient fraction 6 depleted for syndapin II used in in vitro budding assays were obtained by immunoprecipitations with the anti-syndapin II antibody 3685, as described above.

Immunofluorescence microscopy

COS-7 cells were maintained, transfected and processed for immunofluorescence analyses as described previously (Kessels et al., 2001; Kessels and Qualmann, 2002) or incubated for 15 minutes at 37°C with a final concentration of 1 μg brefeldin A (BFA)/ml medium prior to fixation. Incubations with primary antibodies [anti-syndapin II guinea-pig antibody P339, anti-syndapin rabbit antibody 2521 (Qualmann and Kelly, 2000), anti-syntaxin 6 monoclonal antibody, anti-Xpress monoclonal antibody (Invitrogen), anti-Myc monoclonal antibody 9E10 (Babco) and anti-Flag monoclonal antibody M2 (Sigma)], secondary antibodies [Alexa Fluor 488-stained goat anti-guinea-pig antibody (Molecular Probes), Texas Red-conjugated donkey anti-guinea-pig antibody (Dianova), Alexa Fluor 350-stained goat anti-mouse (Molecular Probes), Alexa Fluor 350-stained goat anti-rabbit (Molecular Probes) and Alexa Fluor 568-stained goat anti-mouse antibody (Molecular Probes)] and with MitoTracker® Red CMXRos (Molecular Probes) were performed as described previously (Kessels et al., 2001; Kessels and Qualmann, 2002; Qualmann et al., 2004). The incubations were viewed using a DMR fluorescence microscope (Leica) or an Zeiss Axioplan 2 and 3 microscope, respectively (Zeiss). Images were recorded digitally and processed using Adobe Photoshop software.

Golgi preparation and in vitro formation of transport vesicles

HepG2 cells were metabolically labeled with 0.2 mCi [^{35}S]methionine (Amersham) for 10 minutes at 37°C. After addition of 1 volume DMEM with 0.2 mM methionine, cells were incubated for 1 hour at 20°C to accumulate newly synthesized, labeled proteins in the Golgi. Golgi-enriched membranes were prepared as described and characterized previously (Westermann et al., 1996). They showed, in comparison with total cell membranes, a 150-fold increase in specific activity of galactosyltransferase, a Golgi marker enzyme, determined according to Bretz and Staubli (Bretz and Staubli, 1977). The absence of contaminating ER and plasma membrane was checked, as described previously (Westermann et al., 1996). The absence of endosomes was deduced from a lack of EEA1 immunoblotting signal (anti-EEA1 antibody; Transduction Laboratories). The formation of constitutive transport vesicles was studied in accordance with Tooze and Huttner (Tooze and Huttner, 1992) using Golgi-enriched membranes and cytosolic proteins, as described previously (Dong et al., 2000b). In brief, vesicle formation depends on the addition of cytosol, ATP and GTP. Assays contained Golgi preparations (2 μg protein) that were resuspended in 10 mM HEPES, pH 7.2, 1 mM $MgCl_2$, 1 mM EDTA and 0.25 M sucrose. In some experiments, GST fusion proteins were added at this step and pre-incubated with the Golgi preparations for 15 minutes at 18°C. Thereafter, cytosol (40 μg protein), an ATP-regenerating system and final concentrations of 0.1 mM ATP, 0.1 mM GTP were added. Antisera were dialyzed before addition. Gradient fractions containing the complex of dynamin II with syndapin II were tested in the absence of other cytosolic proteins added. Assays were incubated for 30 minutes at 37°C. Golgi membranes were pelleted (15 minutes at 14,000 ***g***) and thereafter newly formed vesicles were pelleted (20 minutes at 100,000 ***g***). Vesicle preparations have been characterized by isopycnic gradient centrifugation and electron microscopy, as described previously (Westermann et al., 2000). Clathrin, γ-adaptin, rab 6, rab 8 and transferrin receptor were detected as components of constitutive transport vesicles. The absence of GM130 (Westermann et al., 2000), a resident Golgi protein, from vesicle fractions proved that artificial Golgi fragmentation does not occur under our assay conditions.

Golgi membranes and vesicles were solubilized in 1% Triton X-100 and radioactivity was determined. By comparing vesicle labeling with total labeling, the ratios of packaging of labeled proteins into vesicles were calculated. After subtracting background values observed in assays incubated at 0°C, packaging ratios in standard assays were 25-30%. To compare inhibitory effects, packaging ratios under standard conditions were set to 100. The values of at least three independent experiments were used to calculate mean values and standard deviations.

VSVG-GFP trafficking assay

COS-7 cells transfected with VSVG-GFP and VSVG-GFP plus different dynamin and syndapin constructs, respectively, were shifted to 40°C for accumulation of VSVG-GFP in the ER (Presley et al., 1997). BioPorter incubations for antibody introductions were performed as described previously (Kessels and Qualmann, 2002; Braun et al., 2005) directly before the VSVG-GFP transport assay. The VSVG transport assay was essentially performed as described by Cao et al. (Cao et al., 2000). In brief, cells were first incubated with 100 μg/ml cycloheximide for 30 minutes at 40°C. In BioPorter experiments, this time period served as recovery time in serum-containing medium. Thereafter, the VSVG-GFP was released from the ER by shifting the cells to 32°C and cells were subsequently fixed and processed for immunofluorescence microscopy after 0, 15, 45 and 90 minutes. The quantitative evaluation of the transport events towards the plasma membrane was essentially performed as described by Cao et al. (Cao et al., 2000). Images were taken with a CCD camera 2.1.1. from Diagnostic instruments in systematic searches across the coverslips using a 63× Plan Apochromat objective (Zeiss) and constant data acquisition settings. Images were encoded by numbers and transferred to NIH Image software. A perinuclear region of interest with a diameter of 50 pixels (area, 1976 pixels) was positioned and measured by an unbiased experimenter. An average background signal measured on empty areas of the coverslips was subtracted. The samples were then decoded and the measured mean intensity values (given as 255 different gray values) of cells from several independent coverslips were averaged and depicted in an inverted fashion (255-x) so that 255 now represents white and 0 black. The changes of the VSVG-GFP signal in the region of interest over time were depicted as percentage of the values that correspond to the start of the Golgi-to-plasma-membrane chase (i.e. of the time point 15 minutes at 32°C).

The authors are grateful to C. Diatloff-Zito (Institut Curie-Biologie, Paris, France), M. McNiven (Mayo Clinic and Foundation, Rochester, MN), P. McPherson (McGill University, Montreal, Canada) and J. Lippincott-Schwartz (National Institutes of Health, Bethesda, MD), for providing plasmids coding for dynamin II, the SH3 domain of amphiphysin II and VSVG-GFP, respectively. The authors thank M. Knoblich and K. Hartung for skilful technical assistance. This work was supported by grants from the Deutsche Forschungsgemeinschaft to B.Q. (Qu116/2-3), to M.M.K. (Ke685/2-1 and 2-2) and to P.W. (We1482/4-3), as well as from the Kultusministerium of the Land Sachsen-Anhalt (3451A/0502M) to B.Q.

References

Beck, K. A. and Nelson, W. J. (1998). A spectrin membrane skeleton of the Golgi complex. *Biochem. Biophys. Acta* **1404**, 153-160.

Bock, J. B., Klumperman, J., Davanger, S. and Scheller, R. H. (1997). Syntaxin 6 functions in trans-Golgi network vesicle trafficking. *Mol. Biol. Cell* **8**, 1261-1271.

Bonazzi, M., Spanò, S., Turacchio, G., Cericola, C., Valente, C., Colanzi, A., Kweon, H. S., Hsu, V. W., Polishchuck, E. V., Polishchuck, R. S. et al. (2005). CtBP3/BARS drives membrane fission in dynamin-independent transport pathways. *Nat. Cell Biol.* **7**, 570-580.

Braun, A., Pinyol, R., Koch, D., Dahlhaus, R., Fonarev, P., Grant, B. D., Kessels, M. M. and Qualmann, B. (2005). EHD proteins associate with syndapin I and II and such interactions play a crucial role in endosomal recycling. *Mol. Biol. Cell* **16**, 3642-3658.

Bretz, R. and Staubli, W. (1977). Detergent influence on rat-liver galactosyltransferase activities towards different acceptors. *Eur. J. Biochem.* **77**, 181-192.

Cao, H., Garcia, F. and McNiven, M. A. (1998). Differential distribution of dynamin isoforms in mammalian cells. *Mol. Biol. Cell* **9**, 2595-2609.

Cao, H., Thompson, H. M., Krueger, E. W. and McNiven, M. A. (2000). Disruption of Golgi structure and function in mammalian cells expressing a mutant dynamin. *J. Cell Sci.* **113**, 1993-2002.

Cao, H., Weller, S., Orth, J. D., Huang, B., Chen, J. L., Stamnes, M. and McNiven, M. A. (2005). Actin and Arf1-dependent recruitment of a cortactin-dynamin complex to the Golgi regulates post-Golgi transport. *Nat. Cell Biol.* **7**, 483-492.

da Costa, S. R., Sou, E., Xie, J., Yarber, F. A., Okamoto, C. T., Pidgeon, M., Kessels, M. M., Mircheff, A. K., Schechter, J. E., Qualmann, B. et al. (2003). Impairing actin filament or syndapin functions promotes accumulation of clathrin-coated vesicles at the apical plasma membrane of acinar epithelial cells. *Mol. Biol. Cell* **14**, 4397-4413.

De Matteis, M. A. and Morrow, J. S. (2000). Spectrin tethers and mesh in the biosynthetic pathway. *J. Cell Sci.* **113**, 2331-2343.

di Campli, A., Valderrama, F., Babia, T., De Matteis, M. A., Luini, A. and Egea, G. (1999). Morphological changes in the Golgi complex correlate with actin cytoskeleton rearrangements. *Cell Motil. Cytoskeleton* **43**, 334-348.

Dong, J., Misselwitz, R., Welfle, H. and Westermann, P. (2000a). Expression and purification of dynamin II domains and initial studies on structure and function. *Protein Expr. Purif.* **20**, 314-323.

Dong, J., Radau, B., Otto, A., Müller, E., Lindschau, C. and Westermann, P. (2000b). Profilin I attached to the Golgi is required for the formation of constitutive transport vesicles at the trans-Golgi network. *Biochim. Biophys. Acta* **1497**, 253-260.

Fucini, R. V., Chen, J.-L., Sharma, C., Kessels, M. M. and Stamnes, M. (2002). Golgi vesicle proteins are linked to the assembly of an actin complex defined by mAbp1. *Mol. Biol. Cell* **13**, 621-631.

Grabs, D., Slepnev, V. I., Songyang, Z., David, C., Lynch, M., Cantley, L. C. and De Camilli, P. (1997). The SH3 domain of amphiphysin binds the proline-rich domain of dynamin at a single site that defines a new SH3 binding consensus sequence. *J. Biol. Chem.* **272**, 13419-13425.

Griffiths, G., Pfeiffer, S., Simons, K. and Matlin, K. (1985). Exit of newly synthesized membrane proteins from the trans cisterna of the Golgi complex to the plasma membrane. *J. Cell Biol.* **101**, 949-964.

Hinshaw, J. E. (2000). Dynamin and its role in membrane fission. *Annu. Rev. Cell Dev. Biol.* **16**, 483-519.

Jones, S. M., Howell, K. E., Henley, J. R., Cao, H. and McNiven, M. A. (1998). Role of dynamin in the formation of transport vesicles from the trans-Golgi network. *Science* **279**, 573-577.

Kessels, M. M. and Qualmann, B. (2002). Syndapins integrate N-WASP in receptor-mediated endocytosis. *EMBO J.* **21**, 6083-6094.

Kessels, M. M. and Qualmann, B. (2004). The syndapin protein family-linking membrane trafficking with the cytoskeleton. *J. Cell Sci.* **117**, 3077-3086.

Kessels, M. M. and Qualmann, B. (2005). Extending the court for cortactin: from the cortex to the Golgi. *Nat. Cell Biol.* **7**, 448-449.

Kessels, M. M., Engqvist-Goldstein, Å. E. Y., Drubin, D. G. and Qualmann, B. (2001). Mammalian Abp1, a signal-responsive F-actin-binding protein, links the actin cytoskeleton to endocytosis via the GTPase dynamin. *J. Cell Biol.* **153**, 351-366.

Kreitzer, G., Marmorstein, A., Okamoto, P., Vallee, R. and Rodriguez-Boulan, E. (2000). Kinesin and dynamin are required for post-Golgi transport of a plasma-membrane protein. *Nat. Cell Biol.* **2**, 125-127.

Maier, O., Knoblich, M. and Westermann, P. (1996). Dynamin II binds to the trans-Golgi network. *Biochem. Biophys. Res. Commun.* **223**, 229-233.

McNiven, M. A., Cao, H., Pitts, K. R. and Yoon, Y. (2000). The dynamin family of mechanoenzymes: pinching in new places. *Trends Biochem. Sci.* **25**, 115-120.

Müsch, A., Cohen, D., Kreitzer, G. and Rodriguez-Boulan, E. (2001). cdc42 regulates the exit of apical and basolateral proteins from the trans-Golgi network. *EMBO J.* **20**, 2171-2179.

Praefcke, G. J. and McMahon, H. T. (2004). The dynamin superfamily: universal membrane tubulation and fission molecules? *Nat. Rev. Mol. Cell Biol.* **5**, 133-147.

Presley, J. F., Cole, N. B., Schroer, T. A., Hirschberg, K., Zaal, K. J. M. and Lippincott-Schwartz, J. (1997). ER-to-Golgi transport visualized in living cells. *Nature* **389**, 81-85.

Qualmann, B. and Kelly, R. B. (2000). Syndapin isoforms participate in receptor-mediated endocytosis and actin organization. *J. Cell Biol.* **148**, 1047-1061.

Qualmann, B. and Kessels, M. M. (2002). Endocytosis and the cytoskeleton. *Int. Rev. Cytol.* **220**, 93-144.

Qualmann, B., Roos, J., DiGregorio, P. J. and Kelly, R. B. (1999). Syndapin I, a synaptic dynamin-binding protein that associates with the neural Wiskott-Aldrich syndrome protein. *Mol. Biol. Cell* **10**, 501-513.

Qualmann, B., Boeckers T. B., Jeromin, M., Gundelfinger, E. D. and Kessels, M. M. (2004). Linkage of the actin cytoskeleton to the postsynaptic density via interactions of Abp1 with ProSAP/Shanks. *J. Neurosci.*, **24**, 2481-2495.

Qualmann, B., Kessels, M. M. and Kelly, R. B. (2000). Molecular links between endocytosis and the actin cytoskeleton. *J. Cell Biol.* **150**, F111-F116.

Sever, S., Damke, H. and Schmid, S. L. (2000). Garrotes, springs, ratchets, and whips: putting dynamin models to the test. *Traffic* **1**, 385-392.

Simpson, F., Hussain, N. K., Qualmann, B., Kelly, R. B., Kay, B. K., McPherson, P. S. and Schmid, S. L. (1999). SH3-domain-containing proteins function at distinct steps in clathrin-coated vesicle formation. *Nat. Cell Biol.* **1**, 119-124.

Slepnev, V. I. and De Camilli, P. (2000). Accessory factors in clathrin-dependent synaptic vesicle endocytosis. *Nat. Rev. Neurosci.* **1**, 161-172.

Stamnes, M. (2002). Regulating the actin cytoskeleton during vesicular transport. *Curr. Opin. Cell Biol.* **14**, 428-433.

Sweitzer, S. M. and Hinshaw, J. E. (1998). Dynamin undergoes a GTP-dependent conformational change causing vesiculation. *Cell* **93**, 1021-1029.

Tooze, S. A. and Huttner, W. B. (1992). Cell-free formation of immature secretory granules and constitutive secretory vesicles from trans-Golgi network. *Methods Enzymol.* **219**, 81-93.

Valderrama, F., Babia, T., Ayala, I., Kok, J. W., Renau-Piqueras, J. and Egea, G. (1998). Actin microfilaments are essential for the cytological positioning and morphology of the Golgi complex. *Eur. J. Cell Biol.* **76**, 9-17.

Valderrama, F., Durán, J. M., Babià, T., Barth, H., Renau-Piqueras, J. and Egea, G. (2001). Actin microfilaments facilitate the retrograde transport from the Golgi complex to the endoplasmic reticulum in mammalian cells. *Traffic* **2**, 717-726.

Westermann, P., Knoblich, M., Maier, O., Lindschau, C. and Haller, H. (1996). Protein kinase C bound to the Golgi apparatus supports the formation of constitutive transport vesicles. *Biochem. J.* **320**, 651-658.

Westermann, P., Maier, O., Dong, J., Knoblich, M. and Lutsch, G. (2000). Biogenesis and characterization of post-Golgi transport vesicles. *Curr. Top. Biochem. Res.* **3**, 69-80.

Yang, Z., Li, H., Chai, Z., Fullerton, M. J., Cao, Y., Toh, B. H., Funder, J. W. and Liu, J. P. (2001). Dynamin II regulateds hormone secretion in neuroendocrine cells. *J. Biol. Chem.* **276**, 4251-4260.

Journal of Cell Science